European Journal of Mechanics B/Fluids 30 (2011) 589–597

Contents lists available at SciVerse ScienceDirect

European Journal of Mechanics B/Fluids

journal homepage: www.elsevier.com/locate/ejmflu

Recent advances in Serre–Green Naghdi modelling for wave transformation, breaking and runup processes

P. Bonneton [a,*], E. Barthelemy [b], F. Chazel [c], R. Cienfuegos [d], D. Lannes [e], F. Marche [f], M. Tissier [a]

[a] Université Bordeaux 1, CNRS, UMR 5805-EPOC, Talence, F-33405, France
[b] LEGI, INP, BP53 38041 Grenoble Cedex 9, France
[c] Université de Toulouse, UPS/INSA, IMT, CNRS UMR 5219, F-31077 Toulouse, France
[d] Departamento de Ingeniería Hidráulica y Ambiental, Pontificia Universidad Catolica de Chile, Vicuña Mackenna 4860, casilla 306, correo 221, Santiago de Chile, Chile
[e] DMA/CNRS UMR 8553, Ecole Normale Supérieure, 45 rue d'Ulm, 75005 Paris, France
[f] I3M, Université Montpellier 2, CC 051, F-34000 Montpellier, France

ARTICLE INFO

Article history:
Available online 5 March 2011

Keywords:
Water wave
Surf zone
Non-hydrostatic
Boussinesq equations
Saint Venant equations
Finite volume method

ABSTRACT

To describe the strongly nonlinear dynamics of waves propagating in the final stages of shoaling and in the surf and swash zones, fully nonlinear models are required. The ability of the Serre or Green Naghdi (S–GN) equations to reproduce this nonlinear processes is reviewed. Two high-order methods for solving S–GN equations, based on Finite Volume approaches, are presented. The first one is based on a quasi-conservative form of the S–GN equations, and the second on a hybrid Finite Volume/Finite Difference method. We show the ability of these two approaches to accurately simulate nonlinear shoaling, breaking and runup processes.

1. Introduction

Wave propagation in shallow water, and associated processes such as wave-breaking and run-up, play an important role in the nearshore dynamics. The classical and successful method of describing slowly evolving wave-induced circulation in the nearshore is based on the phase-averaged approach, in which the depth-integrated mass and momentum equations are time-averaged over a wave period (see [1]). However, very important unsteady processes, such as wave run-up in the swash zone, coastal flooding during storms, tsunami and tidal bore propagation, require phase-resolving models. For coastal applications, these models are based on nonlinear shallow water equations (NSWE) and Boussinesq-type equations (see [2]). NSWE give a good description of the nonlinear non-dispersive transformation of broken-waves, represented as shocks, in the inner surf and swash zones. However, due to the absence of frequency dispersion, the NSWE can not be applied to wave propagation before breaking. On the other hand, Boussinesq equations incorporate frequency dispersion and can be applied to wave shoaling, but contrary to NSWE they do not implicitly take into account wave breaking. Since the 1990's, significant efforts have been devoted to extend the validity range of Boussinesq equations, by developing wave breaking parametrizations and by improving dispersive properties of these equations. Most Boussinesq models used for nearshore applications are based on classical assumptions of weak nonlinearity, $\epsilon = a/h_0 \ll 1$ (a of the order of free surface amplitude, h_0 the characteristic water depth) and balance between dispersion and nonlinearity: $\epsilon = O(\mu) \ll 1$, where $\mu = (h_0/L)^2$ (L the characteristic horizontal scale). However, these assumptions may severely restrict applicability to real nearshore applications. Indeed, in the final stages of shoaling or in the surf zone, the wave dynamics is strongly nonlinear: $\epsilon = O(1)$. For instance, ϵ is close to 0.4 just before breaking and can be larger than 1 in the swash zone.

In 1953, a breakthrough treating nonlinearity was made by Serre (see [3] for a review). He derived 1D fully nonlinear ($\epsilon = O(1)$) weakly dispersive equations for a horizontal bottom. Green and Naghdi [4] derived 2D fully nonlinear weakly dispersive equations for an uneven bottom which represent a two-dimensional extension of Serre equations (see [5,6]). Except for being formulated in terms of the velocity vector at an arbitrary z level, the equations of Wei et al. [7] are basically equivalent to the 2D Serre or Green–Naghdi equations. It is now recognized that the Serre or Green Naghdi (S–GN) equations represent the relevant system to model highly nonlinear weakly dispersive waves propagating in shallow water (see [8,5]). However, much remains to be done for a proper representation of wave breaking, and for an accurate modeling of moving shorelines over strongly varying topographies.

* Corresponding author.
E-mail address: p.bonneton@epoc.u-bordeaux1.fr (P. Bonneton).

0997-7546/$ – see front matter © 2011 Elsevier Masson SAS. All rights reserved.
doi:10.1016/j.euromechflu.2011.02.005

Due to facility of implementation, early Boussinesq-type models were widely relying on finite difference schemes to discretize the equations (e.g. [9,7]). More recently, spectral approximations [10], Galerkin methods [11], or discontinuous Galerkin methods [12–14] have been successfully applied to KdV-type and some Boussinesq-type models but not to S–GN equations.

Finite volume methods, which are derived on the basis of the integral form of the conservation law, have many advantages. They are conservative and easily formulated to allow for unstructured meshes. Although the finite volume method has been widely and successfully used to solve the strictly hyperbolic NSWE (e.g. [15,2,16]), its application to Boussinesq-type equations has only been reported recently [17–19]. This is related to the fact that finite volume methods essentially aim at a good representation of advection, while methods used for Boussinesq-type equations must also deal with third order derivatives responsible for dispersive effects. To overcome this problem, hybrid approaches, coupling finite volume and the finite difference methods have been recently proposed [20–23]. The hyperbolic terms are treated using shock-capturing methods while the dispersive terms are discretized using the finite difference formulation. Until now, in coastal applications, finite volume and hybrid approaches have only been applied for weakly nonlinear forms of Boussinesq-type equations. However, in the final stages of shoaling and in the surf and swash zones, the effects of nonlinearity are too large to be treated as a small perturbation. In the context of the IDAO ocean research programme we have in the last few years investigated applications of finite volume and hybrid methods to the fully nonlinear weakly dispersive S–GN equations. In this paper, we present a synthesis of this work, emphasizing the ability of S–GN models to deal with wave transformation in the surf and swash zones.

2. Theoretical background

According to [24,5], the 2D S–GN equations can be written in the following non-dimensionalized form

$$\zeta_t + \nabla\cdot(h\mathbf{v}) = 0$$
$$\mathbf{v}_t + \varepsilon(\mathbf{v}\cdot\nabla)\mathbf{v} + \nabla\zeta = -\mu\mathcal{D}, \tag{1}$$

where $\zeta(\mathbf{x},t)$ is the surface elevation, $h(\mathbf{x},t) = 1+\epsilon\zeta - b$ the water depth, $b(\mathbf{x})$ the variation of the bottom topography and $\mathbf{v}(\mathbf{x},t) = (u,v)$ the depth averaged velocity. $\mathcal{D}$ characterizes non-hydrostatic and dispersive effects and writes

$$\mathcal{D} = \mathcal{T}[h,b]\mathbf{v}_t + \varepsilon\left(-\frac{1}{3h}\nabla(h^3((\mathbf{v}\cdot\nabla)(\nabla\cdot\mathbf{v}) - (\nabla\cdot\mathbf{v})^2)) + \mathcal{Q}[h,b](\mathbf{v})\right) \tag{2}$$

where the linear operator $\mathcal{T}[h,b]$ is defined as

$$\mathcal{T}[h,b]W = -\frac{1}{3h}\nabla(h^3\nabla\cdot W) + \frac{1}{2h}[\nabla(h^2\nabla b\cdot W) - h^2\nabla b\nabla\cdot W] + \nabla b\nabla b\cdot W \tag{3}$$

and the purely topographical term $\mathcal{Q}[h,b](\mathbf{v})$ is given by

$$\mathcal{Q}[h,b](\mathbf{v}) = \frac{1}{2h}[\nabla(h^2(\mathbf{v}\cdot\nabla)^2 b) - h^2((\mathbf{v}\cdot\nabla)(\nabla\cdot\mathbf{v}) - (\nabla\cdot\mathbf{v})^2)\nabla b] + ((\mathbf{v}\cdot\nabla)^2 b)\nabla b. \tag{4}$$

The range of validity of this set of equations can be easily extended to wave propagation problems in deeper waters using the dispersion correction technique discussed in Refs. [25–28]. The frequency dispersion properties are improved by applying the operator $I + \mu(\alpha-1)\mathcal{T}[h,b]$ to the momentum equation (1) and neglecting $O(\mu^2)$ terms, which makes the term,

$$(\alpha-1)\mu S = -(\alpha-1)\mu\mathcal{T}[h,b](\mathbf{v}_t + \varepsilon(\mathbf{v}\cdot\nabla)\mathbf{v} + \nabla\zeta), \tag{5}$$

appears on the right-hand side of the momentum equation (1).

The coefficient α is an adjustable parameter that must be tuned in order to minimize the phase and group velocity errors in comparison with the linear Stokes theory. This yields the optimal value $\alpha = 1.159$.[1] Inspired by Nwogu [31], it is also possible to choose another dependent variable (such as the velocity at a certain depth) rather than the mean velocity, as in [7,32]. This allows for more freedom to match the Stokes linear dispersion and/or the exact linear shoaling coefficient. However in that case the mass conservation equation is not exact anymore, but of order $O(\mu^2)$.

It is known that the S–GN equations are mathematically well-posed in the sense that they admit solutions over the relevant time scale for any initial data reasonably smooth (see [33] for the general case, and simpler proofs for one dimensional surfaces [34,35]). Moreover, the solution of the S–GN equations provides a good approximation of the solution of the full water waves equations (see [24] for the general case, and [34] for one dimensional surface waves over flat bottoms); this means that the difference between both solutions remains of order $O(\mu^2)$ as long as the wave does not exhibit any kind of singularity such as wave breaking. Near the breaking point, the relevance of the S–GN equations is a completely open problem since the approximations made to derive the non-hydrostatic and dispersive terms (2) may diverge. Comparison of numerical simulations with experimental data are therefore necessary to assess the validity of the S–GN equations near wave breaking.

The nonlinear shallow water equations (NSWE), or Saint Venant equations, are obtained when the dispersive term $\mu\mathcal{D}$ is neglected in the S–GN equations. It is well known that these nonlinear hyperbolic equations result in discontinuous solutions (shocks), which can be considered as the mathematical counterparts of the breaking wave front. Based on this idea, Hibbert and Peregrine [36] numerically simulated the entire process of bore propagation and runup on a constant beach slope. Kobayashi et al. [37] applied the same approach to simulate the propagation of periodic broken-waves in the surf zone and found good results in comparison with laboratory data. A detailed analysis of the ability of the 1D NSWE shock-wave model to predict cross-shore wave transformation and energy dissipation in the inner surf zone was presented by Bonneton [38]. For 2D problems, Peregrine [39] showed that non-uniformities along the breaking wave front (i.e. along the shock) due to alongshore inhomogeneities in the incident wave field or in the local bathymetry, drive vertical vorticity. Bühler [40] presented a general theoretical analysis of wave-driven currents and vortex dynamics due to dissipating waves. From computations and laboratory measurements, Brocchini et al. [41] and Kennedy et al. [42] showed that breaking-wave-generated vortices are qualitatively well described by the NSWE shock-wave theory. Bonneton et al. [43] emphasized the importance of alongshore inhomogeneities of breaking wave energy dissipation for wave-induced rip current circulation. Their analysis was based on the derivation of an equation for the mean-current vorticity, where the main driving term is related to shock-wave energy dissipation.

The description of shallow water wave dynamics in realistic situations, i.e. over uneven bathymetries from the shoaling zone up to the shoreline, requires the development of advanced numerical

[1] The parameter used in Ref. [30] is given by $\alpha' = (\alpha-1)/3$, with an optimal value $\alpha' = 0.053$.

approaches to integrate fully nonlinear Boussinesq-type equations. In this framework, the S–GN equations offers the quite exceptional property of admitting closed form solutions of the solitary and cnoidal type, bringing the opportunity to assess the accuracy and efficiency of numerical methods.

For horizontal bottoms, the 1D S–GN equations have an exact solitary-wave solution given by, in dimensional variables,

$$h(x,t) = h_0 + H\ \mathrm{sech}^2(\kappa(x-ct)), \tag{6a}$$

$$u(x,t) = c\left(1 - \frac{h_0}{h(x,t)}\right), \tag{6b}$$

$$\kappa = \frac{\sqrt{3H}}{2h_0\sqrt{h_0+H}}, \tag{6c}$$

$$c = \sqrt{g(h+H)}, \tag{6d}$$

where h_0 denotes the mean water depth and H the wave height. This family of solutions is known as the Rayleigh solitary wave solution [44]. Guizien and Barthélémy [45] experimentally checked that solitary waves generated according to Rayleigh's law display very little dispersive trailing waves compared to KdV ones for instance. Li et al. [46] showed numerically that the S–GN solitary solutions are in remarkably close agreement with the exact Euler solutions for large amplitude solitary waves.

Serre [47] showed that the S–GN equations admit also the following family of periodic solutions (see also [48,49]),

$$h(x,t) = a_0 + a_1\mathrm{dn}^2(\kappa(x-ct),k), \tag{7a}$$

$$u(x,t) = c\left(1 - \frac{h_0}{h(x,t)}\right), \tag{7b}$$

$$\kappa = \frac{\sqrt{3a_1}}{2\sqrt{a_0(a_0+a_1)(a_0+(1-k^2)a_1)}}, \tag{7c}$$

$$c = \frac{\sqrt{ga_0(a_0+a_1)(a_0+(1-k^2)a_1)}}{h_0}, \tag{7d}$$

where $k \in [0,1]$, $a_0 > 0$, $a_1 > 0$ are real parameters. In Eq. (7d) $\mathrm{dn}(\cdot,k)$ is a Jacobi elliptic function with elliptic modulus k. This family of solutions constitutes an important extension of the classic KDV cnoidal theory to strongly nonlinear and weakly dispersive applications. It is useful to relate the parameters of this solution to physical variables in order to compute cnoidal waves in terms of wave height, H, wave period, T, and mean water depth, h_0. The latter is achieved by solving the following system of equations [49],

$$a_1 = \frac{H}{k^2} \tag{8a}$$

$$a_0 = h_0 - a_1\frac{E(k)}{K(k)} \tag{8b}$$

$$\hat{\omega}^2 = \frac{3\pi^2 g a_1}{4[a_0K(k) + a_1E(k)]^2} \tag{8c}$$

where $\hat{\omega} = 2\pi/T$ is the angular frequency, $K(k)$ and $E(k)$ are the complete elliptic integrals of the first and second kinds respectively.

As $k \to 1^-$, the family of periodic solutions limits to the two-parameter family of solitary-wave solutions given by Eqs. (6a)–(6d).

3. Reformulations of S–GN equations for numerical implementations

The formulation of the S–GN equations in function of conventional unknowns $(h, \mathbf{v})$, system (1), is not suitable for finite volume methods. In this section, we present two other formulations which are convenient for these numerical methods.

3.1. S–GN equations in a quasi-conservative form

In the 1D case, it is possible to show that continuity and momentum equations can be recast in a weak quasi-conservative form by defining an auxiliary variable q which aggregates all time derivatives in the momentum equations of system (1) [27]. This convenient mathematical form can be written as,

$$\begin{aligned} &h_t + F_x = 0,\\ &q_t + G_x = \alpha'\mu S', \end{aligned} \tag{9}$$

where the source term in the right hand side is related to the small dispersive correction term presented in Section 2,

$$S' = -2\varepsilon(b-1)b_x\partial_x\{uu_x + \zeta_x\}. \tag{10}$$

The auxiliary variable reads,

$$q = \left\{1 + \mu\left[h_xb_x + b_x^2 + \frac{1}{2}hb_{xx} - hh_x\partial_x - \left(\frac{h^2}{3} + \alpha'(b-1)^2\right)\partial_{xx}\right]\right\}u \tag{11}$$

and the functions F and G are defined as follows,

$$\begin{aligned} F &= \varepsilon hu,\\ G &= \varepsilon\left(qu + \zeta - \frac{1}{2}u^2\right) - \mu\varepsilon\left(\frac{1}{2}b_x^2u^2 - hb_xuu_x + \frac{1}{2}h^2u_x^2 + \alpha'(b-1)^2[u_x^2 + uu_{xx} + \zeta_{xx}]\right). \end{aligned}$$

It is important to note that if no dispersion correction is considered (i.e. $\alpha' = 0$) S–GN equations can be written in the form of conservations law even if bottom variations are allowed.

In the framework of numerical modelling, the system (9) can be conveniently integrated over control volumes.

3.2. S–GN equations in terms of the $(h, h\mathbf{v})$ variables

An alternative approach proposed by Bonneton et al. [28] is to write the S–GN equations in terms of the conservative variables $(h, h\mathbf{v})$, namely

$$\begin{aligned} &h_t + \varepsilon\nabla\cdot(h\mathbf{v}) = 0\\ &(h\mathbf{v})_t + \varepsilon\nabla\cdot(h\mathbf{v}\otimes\mathbf{v}) + h\nabla\zeta = -\left(I + \mu\alpha h\mathcal{T}[h,b]\frac{1}{h}\right)^{-1}\\ &\quad\times\left[\frac{1}{\alpha}h\nabla\zeta + \varepsilon\mu h\mathcal{Q}_1[h,b](\mathbf{v})\right] + \frac{1}{\alpha}h\nabla\zeta \end{aligned} \tag{12}$$

with $\mathcal{Q}_1[h,b](\mathbf{v}) = \mathcal{Q}[h,b](\mathbf{v}) - \mathcal{T}[h,b]((\mathbf{v}\cdot\nabla)\mathbf{v})$. It is worth pointing out that this formulation does not include any third-order derivative, allowing for easier and robust numerical computations, especially when the wave becomes steeper. Note that the S–GN equations with improved dispersion à la Nwogu can also be put under a similar form [32].

This formulation is well-suited for a splitting approach with a finite volume method for the hyperbolic part of the equations (the left-hand side of system (12)) and finite difference method for the dispersive part (the right-hand side of system (12)).

4. High-order compact finite volume method

In the 1D case, the quasi-conservative form (9) can be numerically integrated to describe wave propagation in shallow waters.

However, in order to extend the application of the model into the surf zone, additional terms have to be added to the mass and momentum conservation equations. These terms aim at modelling wave-breaking energy dissipation and bottom friction. In dimensional variables, this extended system can be written in the following form,

$$h_t + F_x = D_h,$$
$$q_t + G_x = \frac{1}{h} D_{hu} - \frac{\tau_b}{\rho h} + \alpha' S', \tag{13}$$

where ρ is the water density, D_h and D_{hu} represent breaking terms, τ_b is the bed shear stress.

Breaking-induced energy dissipation mechanisms are introduced through diffusive-like terms, D_h and D_{hu}, applied locally on the wave front face where an explicit breaking criterion is required to switch them on. The mathematical form for D_h and D_{hu} is chosen in order to ensure that the overall mass and momentum budget is preserved, acting only as to locally redistribute these quantities under the breaker [50]. Breaking terms are thus written in the form,

$$D_h = \partial_x(\nu_h h_x),$$
$$D_{hu} = \partial_x(\nu_{hu}(hu)_x),$$

where ν_h and ν_{hu} are diffusivity functions expressed as,

$$\nu_h(X) = -K_h \exp\left(\frac{X}{l_r} - 1\right)\left[\left(\frac{X}{l_r} - 1\right) + \left(\frac{X}{l_r} - 1\right)^2\right],$$
$$\nu_{hu}(X) = -K_{hu} \exp\left(\frac{X}{l_r} - 1\right)\left[\left(\frac{X}{l_r} - 1\right) + \left(\frac{X}{l_r} - 1\right)^2\right],$$

with K_h and K_{hu} slowly varying scaling coefficients, X is a moving horizontal coordinate attached to the wave crest and l_r is the extent over which breaking terms are active. This breaking model has been calibrated on Ting and Kirby's [51] regular wave experiment and optimal parameter values suggested by Cienfuegos et al. [50] are $K_h = 2cd$, $K_{hu} = 20cd$ and $l_r/d = 0.82$, with $c = (gd)^{0.5}$ and d the local still water depth.

The numerical integration of the system (13) is performed using a high-order compact finite volume method. A detailed description of this model, SERR-1D, is given in Refs. [27,30]. The equations are first integrated in space over discrete control volumes $\Omega_i = \{x \in [x_{i-\frac{1}{2}}, x_{i+\frac{1}{2}}]\}$,

$$\frac{\partial}{\partial t}\int_{x_{i-\frac{1}{2}}}^{x_{i+\frac{1}{2}}} h\,\mathrm{d}x + F(x_{i+\frac{1}{2}}, t) - F(x_{i-\frac{1}{2}}, t) = \int_{x_{i-\frac{1}{2}}}^{x_{i+\frac{1}{2}}} \partial_x(\nu_h h_x)\,\mathrm{d}x, \tag{14}$$

$$\frac{\partial}{\partial t}\int_{x_{i-\frac{1}{2}}}^{x_{i+\frac{1}{2}}} q\,\mathrm{d}x + G(x_{i+\frac{1}{2}}, t) - G(x_{i-\frac{1}{2}}, t) = \int_{x_{i-\frac{1}{2}}}^{x_{i+\frac{1}{2}}} \left(S' + \frac{1}{h}\partial_x(\nu_{hu}(hu)_x) - \frac{\tau_b}{\rho h}\right)\mathrm{d}x, \tag{15}$$

where the integral of variables h and q over control volumes must be advanced in time. The average value of function h at time $t = t_n$ over control volume Ω_i is noted as,

$$\widehat{h}_i^n = \frac{1}{\Delta x}\int_{x_{i-\frac{1}{2}}}^{x_{i+\frac{1}{2}}} h(x, t_n)\,\mathrm{d}x$$

where $\Delta x = x_{i+\frac{1}{2}} - x_{i-\frac{1}{2}}$ is the length of the discrete control volumes. Hence, integrated over the whole domain, Eqs. (14) and (15) can be expressed as,

$$\frac{\mathrm{d}\widehat{h}_i^n}{\mathrm{d}t} = -\frac{1}{\Delta x}(F^n_{i+\frac{1}{2}} - F^n_{i-\frac{1}{2}} - \{\nu_h h_x\}|_{i+\frac{1}{2}} + \{\nu_h h_x\}|_{i-\frac{1}{2}}),$$
$$\frac{\mathrm{d}\widehat{q}_i^n}{\mathrm{d}t} = \widehat{S}_i^n - \frac{1}{\Delta x}(G^n_{i+\frac{1}{2}} - G^n_{i-\frac{1}{2}}), \quad \text{for } i = 1, 2, \ldots, N,$$

where N is the total number of control volumes used to discretize the physical domain and $\widehat{S}_i^n$ is the discretized counterpart of the source term in the right hand side of Eq. (15). This term is approximated through centred finite differences. The values h and q at cell interfaces are reconstructed from cell-averaged values using the implicit 4th order compact interpolation technique described in Refs. [52,53]. At each time step, the velocity component at control volume interfaces is computed numerically by inverting Eq. (11). Time stepping is performed through a 4th order Runge–Kutta method.

Efficient absorbing–generating boundary conditions have been implemented in SERR-1D. They are based on the following characteristic form of the S–GN equations,

$$\frac{\mathrm{d}R^+}{\mathrm{d}t} = -\frac{1}{3h}\frac{\partial}{\partial x}(h^2 P) - g b_x - \frac{\tau_b}{\rho h} \quad \text{along } \frac{\mathrm{d}x}{\mathrm{d}t} = u + \sqrt{gh}, \tag{16}$$

$$\frac{\mathrm{d}R^-}{\mathrm{d}t} = -\frac{1}{3h}\frac{\partial}{\partial x}(h^2 P) - g b_x - \frac{\tau_b}{\rho h} \quad \text{along } \frac{\mathrm{d}x}{\mathrm{d}t} = u - \sqrt{gh}, \tag{17}$$

with positive and negative Riemann variables defined respectively as $R^+ = u + 2\sqrt{gh}$ and $R^- = u - 2\sqrt{gh}$. Vertical acceleration of fluid particles, which is of order $O(\mu)$ and thus disregarded in the nonlinear shallow water equations (NSWE), is represented by function P in the first term of the right hand side of Eqs. (16)–(17). This term is responsible for the loss of hyperbolicity in the S–GN equations by introducing an horizontal dependence in the characteristic plane (x, t).

It is worth noting that from a physical point of view we can expect that time scales associated with dispersive effects would be larger than the ones associated with nonlinearities from intermediate to shallow waters. We may therefore assume that over short distances/times, Riemann variables might be locally conserved along characteristics. This physical argument has been used to develop absorbing–generating boundary conditions for the numerical resolution of S–GN equations [30,54].

For the moving shoreline boundary condition, the simple extrapolation technique proposed by Lynett et al. [55] has been adapted in the finite volume resolution.

SERR-1D has been extensively validated by comparisons with non-breaking and breaking wave laboratory experiments [56,30,50,54].

In the present paper, the capabilities of the model are illustrated by comparing numerical computations with breaking random wave propagation experiments. We use measurements conducted at the 70-m long wave tank of the Instituto Nacional de Hidraulica (Chile), prepared with a beach of a very mild slope of 1/80 in order to produce large surf zone extensions [57]. A random JONSWAP type wave field ($h_0 = 0.52$ m, $f_p = 0.25$ Hz, $H_{mo} = 0.17$ m) was generated by a piston wave-maker and measurements of the free surface displacements were performed all over its length at high spatial resolution (0.2–1 m). This experiment allows us to test numerical models that are assumed to reproduce nonlinear shallow water wave propagation, breaking and run-up. The evolution of the wave energy power spectral density as the wave field propagates over the beach is presented in Fig. 1, for both experimental measurements and numerical results. SERR-1D is able to simulate the complex nonlinear energy transfer occurring in the shoaling and surf zones. In particular, it reproduces the generation of higher frequency harmonics during shoaling (between $x = -9$ m and $x = 9$ m), energy dissipation by breaking in the surf zone (between $x = 9$ m and $x = 32$ m). The numerical results also indicate that the model is able to reproduce the energy transfer from the Jonswap spectrum band (>0.1 Hz) to the infragravity band (<0.1 Hz). It is important to note that the numerical model was forced with the high-pass filtered wave signal measured 2 m away from the wave paddle without energy

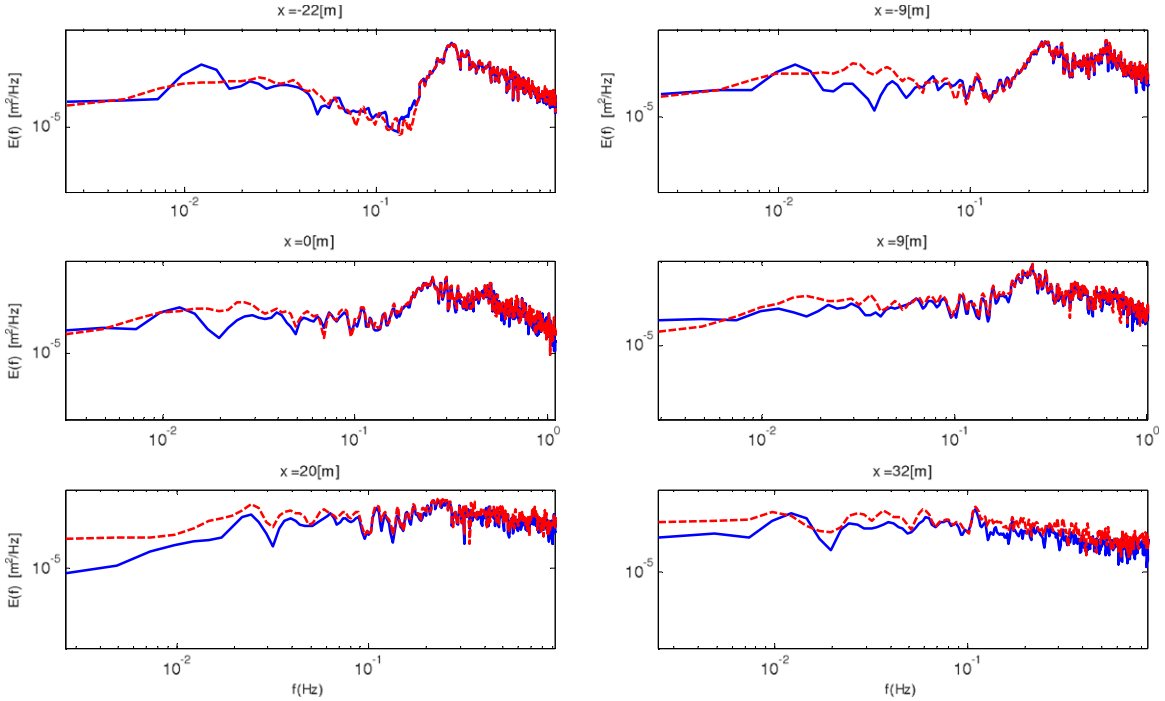

Fig. 1. Random wave transformation and breaking over a mild slope beach. The origin of the x-coordinate is at the toe of the beach slope, positive towards the shore. Solid line: experimental data; dashed line: computed results.

content in the infragravity band. Observed differences in the infragravity band frequencies might be attributed to differences in the wave tank seaward boundary condition (wave paddle and semi-enclosed basin producing partial reflection of long waves at the wave paddle) and the effective open seaward boundary condition used in SERR-1D (see [58]).

5. High-order hybrid finite volume/finite difference method

The formulation of S–GN equations introduced in Section 3 (Eqs. (12)) is well-suited for a splitting approach separating the hyperbolic and the dispersive part of the equations. In this section, we first present an efficient high-order positive preserving well-balanced shock-capturing scheme for the hyperbolic step and then the splitting method for solving the whole S–GN system.

5.1. NSWE shock capturing solver

We consider in this section the hyperbolic part of the S–GN equation, stated in the dimensionalized form:

$$h_t + \nabla\cdot(h\mathbf{v}) = 0 \qquad (18)$$
$$(h\mathbf{v})_t + \nabla\cdot(h\mathbf{v}\otimes\mathbf{v}) + gh\nabla\zeta = 0.$$

This system can be also regarded as a hyperbolic system of conservation laws with a geometrical source term controlled by the topography variations. To simplify the algorithm presentation we only consider the one-dimensional problem:

$$\mathbf{w}_t + f(\mathbf{w})_x = S(\mathbf{w}), \qquad (19)$$

where $\mathbf{w} = {}^t(h, hu)$, $f(\mathbf{w}) = {}^t(hu, hu^2 + 0.5gh^2)$ and $S = {}^t(0, -ghb_x)$ is the source term. To perform numerical approximations of the weak solutions of this system, we use a high order finite-volume approach in conservative variables, relying on Riemann problems for hyperbolic conservative laws [59]. This approach allows accurate computation of propagating bores, with reduced spurious effects of numerical dissipation and dispersion. Using such an accurate scheme, we are able to handle wave breaking (see Section 2). Since we aim at computing the complex interactions between propagating waves and topography (including the preservation of motionless steady states), we also embed this approach into a well-balanced scheme.

More precisely, based on discrete finite-volume cell averaging $\bar{\mathbf{w}}_i^n$ at time $t^n = n\Delta t$, we use the limited 4th-order MUSCL reconstruction suggested in [60]. Considering a cell C_i, this approach provides, for all t^n, high order accuracy interpolated quantities $\bar{\mathbf{w}}_{i,l}$ and $\bar{\mathbf{w}}_{i,r}$, respectively at the left and right boundary of each cell. To get a positive preserving and well-balanced scheme, additional faces reconstructions are introduced [61]:

$$b_i^* = \max(b_{i,r}, b_{i+1,l}),$$
$$h_{i,r}^* = \max(0, h_{i,r} + b_{i,r} - b_i^*),$$
$$h_{i+1,l}^* = \max(0, h_{i+1,l} + b_{i+1,l} - b_i^*).$$

These new left and right values for water height are used to compute auxiliary conservative faces values $\mathbf{w}_{i,r}^*$ and $\mathbf{w}_{i+1,l}^*$:

$$\mathbf{w}_{i,r}^* = \begin{pmatrix} h_{i,r}^* \\ h_{i,r}^* u_{i,r} \end{pmatrix}, \qquad \mathbf{w}_{i+1,l}^* = \begin{pmatrix} h_{i+1,l}^* \\ h_{i+1,l}^* u_{i+1,l} \end{pmatrix} \qquad (20)$$

which are injected into a Riemann solver. Neglecting temporally the time discretization, we obtain the following semi-discrete finite-volume scheme for (19):

$$\frac{\mathrm{d}}{\mathrm{d}t}\bar{\mathbf{w}}_i(t) + \frac{1}{\Delta x}\left(\mathbf{f}_{i+\frac{1}{2}}(\bar{\mathbf{w}}_{i,r}, \bar{\mathbf{w}}_{i+1,l}, b_{i,r}, b_{i+1,l}) - \mathbf{f}_{i-\frac{1}{2}}(\bar{\mathbf{w}}_{i-1,r}, \bar{\mathbf{w}}_{i,l}, b_{i-1,r}, b_{i,l})\right) = S_{c,i}$$

where $\mathbf{f}_{i+\frac{1}{2}}$ and $\mathbf{f}_{i-\frac{1}{2}}$ are the numerical flux functions based both on a conservative flux consistent with the homogeneous NSWE issued from a relaxation approach [60], and the hydrostatic reconstruction correction to the interface fluxes [61]. $S_{c,i}$ is a centered discretization of the source term needed to achieve accuracy, consistency and well-balancing properties.

The resulting finite-volume scheme provides high-order accuracy approximations of the weak solutions of system (19) while

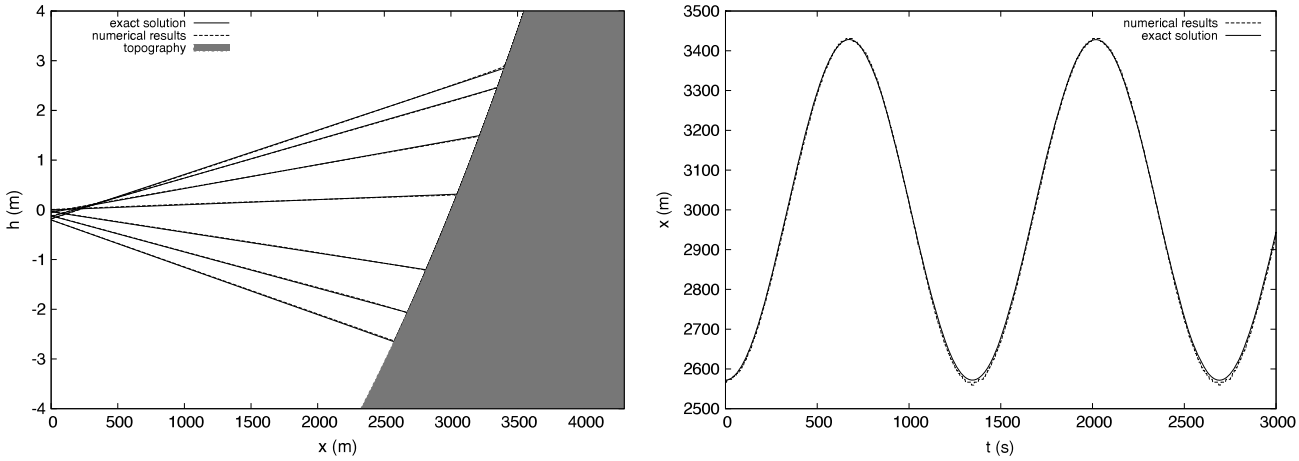

Fig. 2. (a) Free surface at various time between a half evolution period (analytical solution in solid line). (b) Shoreline location between $t = 0$ s and $t = 3000$ s.

preserving the positivity of the water-height, thanks to the relaxation approach developed in [60]. This last property is paramount to ensure robust and accurate simulations of time-evolving shorelines [16]. In addition, the use of a well-balanced scheme leads to accurate computations of incident waves and topography complex interactions classically occurring in the surf zone [62]. It also allows far more accurate results in situations involving tiny oscillations near steady states. The resulting high-order positive preserving well-balanced shock-capturing scheme was implemented in the code SURF-WB [16,60].

We can observe in Fig. 2 a comparison between numerical results and analytical solutions for a one dimensional test case. This solution describes time oscillations of a forced flow over a quadratic topography profile, involving a moving shoreline [63]. The free surface is always planar during the oscillations. The computational domain is 4320 m long and the topography is given by

$$b(x) = 1 - h_0 \left(\frac{x}{a}\right)^2$$

where $h_0 = 10$ m and $a = 3000$ m are respectively the mean water depth and a topography scaling parameter. The flow motion is driven by the left boundary condition, where we impose a periodic motion:

$$h(t,0) = -\frac{a^2 B^2}{8g^2 h_0}\left(\frac{8gh_0}{a^2}\cos(2\sqrt{8gh_0/a^2}\,t)\right) - \frac{B^2}{4g} \tag{21}$$

where B is a free parameter, set to 2 m s^{-1} for the simulation shown here. Note that the shoreline location, x_s, can be analytically derived:

$$x_s = \frac{a^2}{2gh_0}(-B\sqrt{8gh_0/a^2}\cos(\sqrt{8gh_0/a^2}\,t)) + a.$$

The simulation has been performed with 200 cells and the time step is set to 0.03 s, with a first order scheme. Results are shown first as a comparison between numerical results and analytical NSWE solutions for the free surface elevation, at several times. Note that the results and the solution are almost indistinguishable. Then we highlight the accuracy of the shoreline location prediction through a comparison between analytical and numerically predicted shoreline locations, for a period of 3000 s.

5.2. S–GN splitting solver

Eqs. (12) are solved using the following splitting method: we decompose the solution operator $S(\cdot)$ associated to (12) at each time step by the second order splitting scheme

$$S(\Delta t) = S_1(\Delta t/2)S_2(\Delta t)S_1(\Delta t/2), \tag{22}$$

where $S_1(t)$ is the solution operator associated with the nonlinear shallow water equations (18), while $S_2(t)$ is the solution operator associated with the dispersive part of the equations, namely

$$\begin{cases} h_t = 0, \\ (hV)_t = -\left(I + \alpha h\mathcal{T}\dfrac{1}{h}\right)^{-1}\left[\dfrac{1}{\alpha}gh\nabla\zeta + h\mathcal{Q}_1(V)\right] + \dfrac{1}{\alpha}gh\nabla\zeta. \end{cases} \tag{23}$$

As described previously, $S_1(t)$ is computed using a finite-volume approach, while a finite-difference approach is used to solve $S_2(t)$ at each time step: the spatial derivatives are discretized using centered fourth-order formulae. Boundary conditions are imposed using the method presented in [28]. As far as time discretization is concerned, we choose to solve $S_1(t)$ and $S_2(t)$ using an explicit fourth-order Runge–Kutta scheme.

To sum up, $S_1(t)$ and $S_2(t)$ are solved, within our splitting approach, using a fourth-order scheme in space and time. However, the use of a second-order splitting method implies that the global scheme is of order two in time. The use of a fourth-order Runge–Kutta scheme for $S_1(t)$ and $S_2(t)$ is however required to have a good semi-discrete dispersion relation. A detailed description of the new S–GN splitting solver implemented in the SURF-WB code is given in [28].

In order to handle wave breaking, we switch from the S–GN equations to the NSWE, locally in time and space, by skipping the dispersive step $S_2(\Delta t)$ when the wave is ready to break. In this way, we only solve the hyperbolic part of the equations for the wave fronts, and the breaking wave dissipation is represented by the shock energy dissipation (see also [38]). To determine where to suppress the dispersive step at each time step, we use the first half-time step S_1 of the time-splitting as a predictor to assess the local energy dissipation. This dissipation is close to zero in regular wave regions, and forms a peak when shocks are appearing. We can then easily locate the eventual breaking wave fronts at each time step, and skip the dispersive step only at the wave fronts (see [64]).

6. Validation

In this section, the capabilities of the two models, SERR1D and SURF-WB, are evaluated by comparing numerical computations with both analytical solutions and laboratory measurements.

In order to test the efficiency of our approaches to simulate nonlinear waves, the propagation of a strongly non-linear cnoidal wave solution of the S–GN equations (see relations (7d)) is investigated. Periodic boundary conditions have been used in order to appreciate the propagation of the cnoidal wave over a long period, and the computational domain length is equal to the

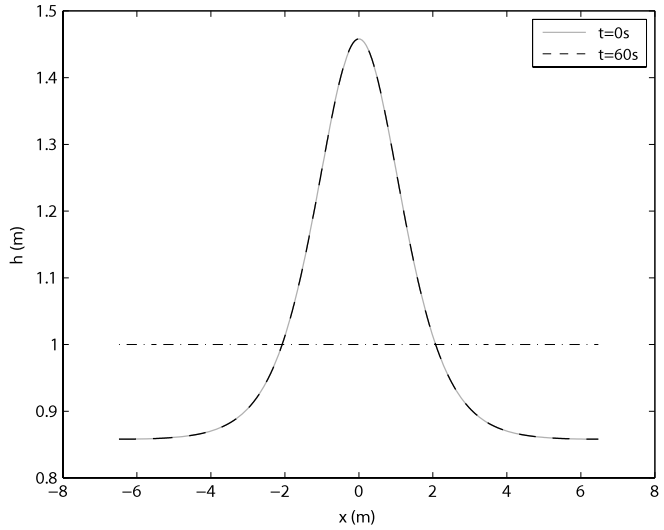

Fig. 3. Propagation of a strongly nonlinear cnoidal wave ($H = 0.6$ m, $h_0 = 1$ m, $T = 4$ s) over a periodic domain. Solid line: solution at $t = 0$; dashed line: numerical solution computed with SURF-WB at $t = 15T = 60$ s; doted line: still water level. $\Delta x = 0.01$ m and the Courant number is equal to 1.

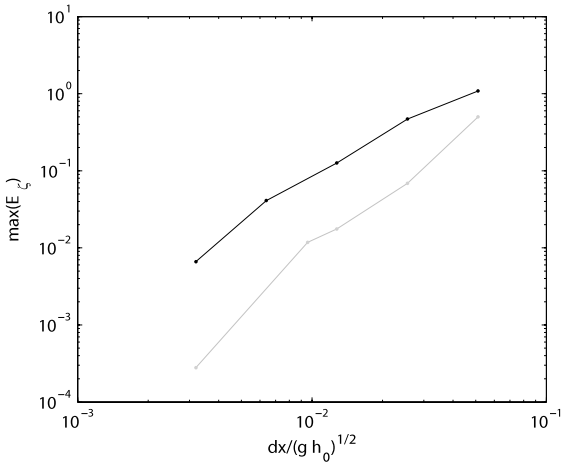

Fig. 4. Discretization errors for the numerical solution of a strongly nonlinear cnoidal wave ($H = 0.6$ m, $h_0 = 1$ m, $T = 4$ s). Convergence error in $\Delta x/(gh_0)^{1/2}$ at $t = 15T$ using a fixed $\Delta t = 0.0032$ s. black line : SERR1D, grey line: SURF-WB.

cnoidal wave-length. The initial condition is a cnoidal wave with $H = 0.6$ m, $h_0 = 1$ m and $T = 4$ s (see Fig. 3). Numerical and theoretical solutions are compared at $t = 15T = 60$ s for different cell sizes, while keeping Δt equal to 0.0032 s. Fig. 3 shows SURF-WB results for the finest grid size considered ($\Delta x = 0.01$ m). The cnoidal wave solutions at $t = 0$ s and $t = 60$ s are both plotted in this figure, but cannot be distinguished since the errors on wave height and celerity are extremely small (relative amplitude error of 3.1×10^{-5} and relative celerity error smaller than 5.4×10^{-3}). Convergence curves for both models are presented in Fig. 4. The relative error E_ζ on the free surface elevation is computed using the discrete L^∞ norm $\|.\|_\infty$:

$$E_\zeta = \frac{\|h_{num} - h_{sol}\|_\infty}{\|h_{sol} - h_0\|_\infty};$$

where h_{num} are the numerical solutions and ζ_{sol} denotes the analytical ones coming from (7d). SURF-WB gives slightly more accurate solutions than SERR1D. The observed order of accuracy is 2.61 for SURF-WB and 1.82 for SERR1D. For less demanding tests in term of nonlinearity, [27] showed that the order of accuracy of SERR1D is close to the theoretical one $O(\Delta x^4)$.

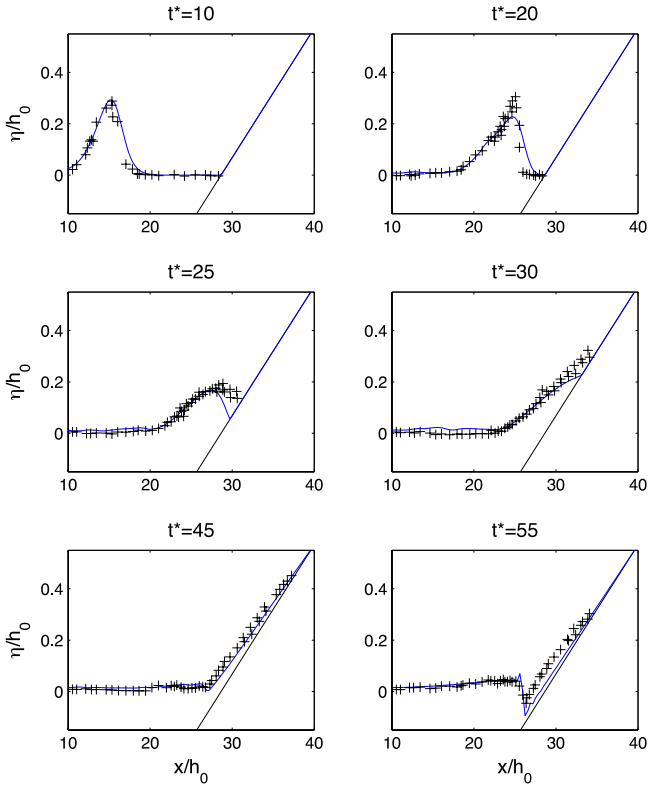

Fig. 5. Comparisons of SERR1D predictions (−) and experimental data (+) for a breaking solitary wave with non-dimensional initial incident amplitude $a_0/h_0 = 0.28$, on a 1:19.85 constant slope beach investigated by Synolakis [65]. $t^* = t(g/h_0)^{1/2}$.

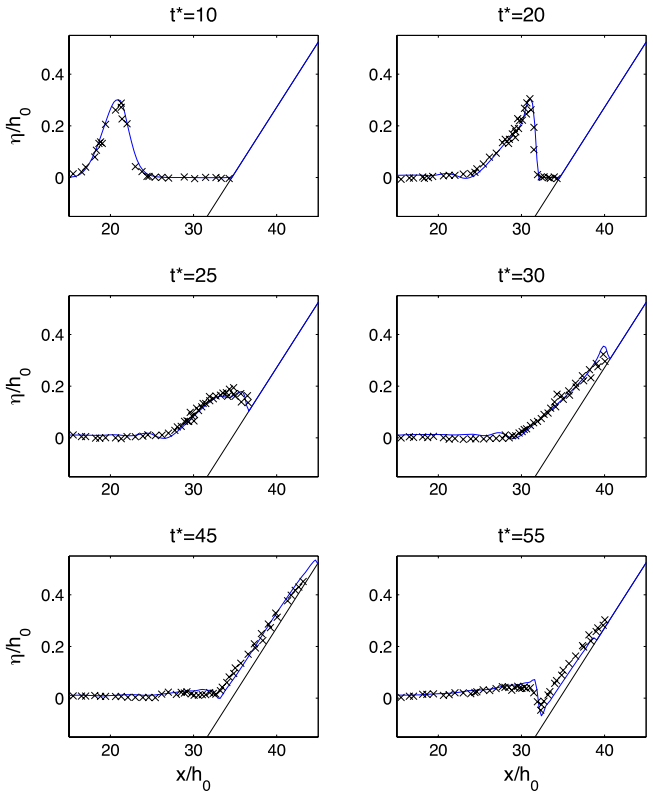

Fig. 6. Comparisons of SURF-WB predictions (−) and experimental data (x) for a breaking solitary wave with non-dimensional initial incident amplitude $a_0/h_0 = 0.28$, on a 1:19.85 constant slope beach investigated by Synolakis [65]. $t^* = t(g/h_0)^{1/2}$.

Fig. 7. Tidal bore propagation in Garonne River; Mascaret project (see [29]).

In the next case, we assess the ability of our models to describe wave runup and breaking, by comparing their numerical solutions to laboratory experiments carried out by Synolakis [65], for an incident solitary wave of relative amplitude $a_0/h_0 = 0.28$, propagating and breaking over a planar beach with a slope of 1:19.85. The still water level in the horizontal part of the beach was $h_0 = 0.3$ m, and the simulations are performed using the grid size $\Delta x = 0.08$ m and $\Delta t = 0.02$ s.

The comparisons between measured and computed waves are presented in Fig. 5 for SERR1D and Fig. 6 for SURF-WB. In both cases, we observe a good agreement between model predictions and laboratory data for the wave shoaling, breaking, run-up and run-down. In particular, we note the good ability of SURF-WB to describe the formation and breaking of a backwash bore, which is a particularly demanding test for most of Boussinesq-type models, since it involves broken bore propagating backward.

7. Conclusion

As the waves approach the shore, the nonlinearity effects become intense, especially in the final stages of shoaling and the surf zone. To simulate such nonlinear processes in shallow water, fully nonlinear Boussinesq-type approaches are required. The Serre or Green Naghdi (S–GN) equations, with improved dispersion properties, represent the relevant system to model these highly nonlinear weakly dispersive waves (see [5]). Two high-order methods for solving S–GN equations, based on Finite Volume approaches, are presented in this article.

The first one is based on a quasi-conservative form of the S–GN equations. Wave-breaking energy dissipation is taken into account through a diffusive-type parametrization on both the mass conservation and momentum conservation [50]. This model, SERR-1D, has been extensively validated by multiple comparisons between numerical simulations and physical experiments including solitary waves shoaling, regular waves propagating over a submerged bar [30] or regular wave breaking over uniform beach slopes [50]. In the present paper, new results show the ability of the model to reproduce nonlinear energy transfer for random waves, in the shoaling and surf zones.

We present also an alternative approach where the S–GN equations are reformulated in terms of the conservative variables $(h, h\mathbf{v})$ (Eqs. (12)). This formulation is well-suited for a splitting approach with a finite volume method for the hyperbolic part of the S–GN equations (NSWE) and a finite difference method for the dispersive part [28]. Our hyperbolic method is based on a high-order well-balanced shock-capturing scheme [16,60]. In the present article we show that our hybrid model, SURF-WB, accurately describes strongly nonlinear S–GN cnoidal wave solutions. In order to handle wave breaking, we switch locally from the S–GN equations to the hyperbolic NSWE, where the wave is ready to break. In this way, we only solve the hyperbolic part of the equations for the wave fronts, and the breaking wave dissipation is represented by shock energy dissipation. We show that this approach accurately predicts nonlinear shoaling, breaking and runup of solitary waves on a beach. The advantage of this approach, in comparison with classical breaking parametrizations, is that it is easily extended to 2DH broken-wave problems. This is crucial to predict wave-induced circulations and macro-vortices, which are strongly controlled by dissipation non-uniformities along broken-wave fronts [2,43].

Further work is required to evaluate the capability of our S–GN models to predict such 2DH flows. An another important open problem concerns the ability of our approaches to predict bore dynamics in a large range of Froude numbers, from "non-breaking undular bore" to "breaking bore". The transition between those two types of bores, which is controlled by the competition between nonlinearity, dispersion and dissipation effects, is still poorly understood. Recent field experiments on the dynamics of tidal bores (see Fig. 7) will give us the opportunity to validate our models.

Acknowledgements

The authors would like to acknowledge the financial and scientific support of the French INSU — CNRS (Institut National des Sciences de l'Univers — Centre National de la Recherche Scientifique) program IDAO ("Interactions et Dynamique de l'Atmosphère et de l'Océan"). This work has also been supported by the ANR MathOcean, the ANR MISEEVA and the project ECOS-CONYCIT action C07U01.

References

[1] O.M. Phillips, The Dynamics of the Upper Ocean, second edition, Cambridge University Press, 1977.
[2] M. Brocchini, N. Dodd, Nonlinear shallow water equation modeling for coastal engineering, J. Waterway Port Coast Ocean Eng. 134 (2) (2008) 104–120.
[3] E. Barthélemy, Nonlinear shallow water theories for coastal waves, Surv. Geophys. 25 (2004) 315–337.
[4] A.E. Green, P.M. Naghdi, A derivation of equations for wave propagation in water of variable depth, J. Fluid Mech. 78 (2) (1976) 237–246.
[5] D. Lannes, P. Bonneton, Derivation of asymptotic two-dimensional time-dependent equations for surface water wave propagation, Phys. Fluids 21 (1) (2009) 016601. doi:10.1063/1.3053183. (9 pages).
[6] F. Dias, P. Milewski, On the fully non-linear shallow-water generalized Serre equations, Phys. Lett. A 374 (2010) 1049–1053.
[7] G. Wei, J.T. Kirby, S.T. Grilli, R. Subramanya, A fully nonlinear Boussinesq model for surface waves. Part 1. Highly nonlinear unsteady waves, J. Fluid Mech. 294 (1995) 71–92.
[8] F.J. Seabra-Santos, D.P. Renouard, A.M. Temperville, Numerical and experimental study of the transformation of a solitary wave over a shelf or isolated obstacle, J. Fluid Mech. 176 (1987) 117–134.
[9] M.B. Abbott, A.D. McCowan, I.R. Warren, Accuracy of short-wave numerical model, J. Hydraul. Res. 110 (10) (1984) 1287–1301.
[10] M. Chen, Numerical investigation of a two-dimensional Boussinesq system, Discrete Contin. Dyn. Syst. 28 (4) (2009) 1169–1190.

[11] P. Avilez-Valente, F. Seabra-Santos, A high-order Petrov–Galerkin finite element method for the classical Boussinesq wave model, Int. J. Numer. Methods Fluids 59 (9) (2009) 969–1010.
[12] J. Yan, C.-W. Shu, A local discontinuous Galerkin method for KdV type equations, SIAM J. Numer. Anal. 40 (2) (2002) 769–791.
[13] H. Liu, J. Yan, A local discontinuous Galerkin method for the Korteweg–de Vries equation with boundary effect, J. Comput. Phys. 215 (2006) 197–218.
[14] C. Eskilsson, S.-J. Sherwin, Spectral/hp discontinuous Galerkin method for modelling 2D Boussinesq equations, J. Comput. Phys. 212 (2) (2006) 566–589.
[15] R.J. LeVeque, Finite Volume Methods for Hyperbolic Problems, Cambridge University Press, 2002.
[16] F. Marche, P. Bonneton, P. Fabrie, N. Seguin, Evaluation of well-balanced bore-capturing schemes for 2D wetting and drying processes, Int. J. Numer. Methods Fluids 53 (5) (2007) 867–894.
[17] S.F. Bradford, B.F. Sanders, Finite-volume models for unidirectional, nonlinear, dispersive waves, J. Waterway Port Coast Ocean Eng. 128 (4) (2002) 173–182.
[18] P.K. Stansby, Solitary wave run up and overtopping by a semi-implicit finite-volume shallow-water Boussinesq model, J. Hydraul. Res. 41 (6) (2003) 639–647.
[19] F. Benkhaldoun, M. Seaid, New finite-volume relaxation methods for the third-order differential equations, Commun. Comput. Phys. 4 (4) (2008) 820–837.
[20] S. Soares Frazao, Y. Zech, Undular bores and secondary waves — experiments and hybrid finite-volume modelling, J. Hydraul. Res. 40 (2002) 33–43.
[21] R. Bernetti, E.F. Toro, M. Brocchini, An operator-splitting method for long waves, Long Waves Symposium, Thessaloniki, Greece 1 (2003) 49–56.
[22] KS Erduran, S Ilic, V. Kutija, Hybrid finite-volume finite-difference scheme for the solution of Boussinesq equations, Int. J. Numer. Methods Fluids 49 (11) (2005) 1213–1232.
[23] O. Le Métayer, S. Gavrilyuk, S. Hank, A numerical scheme for the Green–Naghdi model, J. Comput. Phys. 229 (2010) 2034–2045.
[24] B. Alvarez-Sameniego, D. Lannes, Large time existence for 3D water waves and asymptotics, Invent. Math. 171 (2008) 485–541.
[25] J.M. Witting, A unified model for the evolution of nonlinear water waves, J. Comput. Phys. 56 (2) (1984) 203–236.
[26] P.A. Madsen, R. Murray, O.R. Sorensen, A new form of the Boussinesq equations with improved linear dispersion characteristics, Coast. Eng. 15 (1991) 371–388.
[27] R. Cienfuegos, E. Barthelemy, P. Bonneton, A fourth-order compact finite volume scheme for fully nonlinear and weakly dispersive Boussinesq-type equations. Part I: model development and analysis, Int. J. Numer. Methods Fluids 56 (2006) 1217–1253.
[28] P. Bonneton, F. Chazel, D. Lannes, F. Marche, M. Tissier, A splitting approach for the fully nonlinear and weakly dispersive Green–Naghdi model, J. Comput. Phys. 230 (4) (2011) 1479–1498. doi:10.1016/j.jcp.2010.11.015.
[29] P. Bonneton, J. Van de Loock, J-P. Parisot, N. Bonneton, A. Sottolichio, G. Detandt, B. Castelle, V. Marieu, N. Pochon, 2011 On the occurrence of tidal bores - The Garonne River case. J Coast. Res., SI 64, (in press).
[30] R. Cienfuegos, E. Barthelemy, P. Bonneton, A fourth-order compact finite volume scheme for fully nonlinear and weakly dispersive Boussinesq-type equations. Part II: boundary conditions and model validation, Int. J. Numer. Methods Fluids 53 (9) (2007) 1423–1455.
[31] O. Nwogu, Alternative form of boussinesq equations for nearshore wave propagation, J. Waterway Port Coast Ocean Eng. 119 (1993) 616–638.
[32] F. Chazel, D. Lannes, F. Marche, Numerical simulation of strongly nonlinear and dispersive waves using a Green–Naghdi model, J. Sci. Comput. (2010) doi:10.1007/s10915-010-9395-9.
[33] B. Alvarez-Samaniego, D. Lannes, A Nash–Moser theorem for singular evolution equations. Application to the Serre and Green–Naghdi equations, Indiana Univ. Math. J. 57 (1) (2008) 97–131.
[34] Y.A. Li, A shallow-water approximation to the full water wave problem, Commun. Pure Appl. Math. 59 (9) (2006) 1225–1285.
[35] S. Israwi, Large Time existence For 1D Green–Naghdi equations, 2009, preprint arXiv:0909.2232v1.
[36] S. Hibbert, D.H. Peregrine, Surf and run-up on a beach: a uniform bore, J. Fluid Mech. 95 (1979) 323–345.
[37] N. Kobayashi, G. De Silva, K. Watson, Wave transformation and swash oscillation on gentle and steep slopes, J. Geophys. Res. 94 (1989) 951–966.
[38] P. Bonneton, Modelling of periodic wave transformation in the inner surf zone, Ocean Eng. 34 (2007) 1459–1471.
[39] D.H. Peregrine, Surf zone currents, Theor. Comput. Fluid Dyn. 10 (1998) 295–309.
[40] O. Bühler, On the vorticity transport due to dissipating or breaking waves in shallow-water flow, J. Fluid Mech. 407 (2000) 235–263.
[41] M. Brocchini, A. Kennedy, L. Soldini, A. Mancinelli, Topographically controlled, breaking-wave-induced macrovortices. Part 1. Widely separated breakwaters, J. Fluid Mech. 507 (2004) 289–307.
[42] A.B. Kennedy, M. Brocchini, L. Soldini, E. Gutierrez, Topographically controlled, breaking-wave-induced macrovortices. Part 2. Changing geometries, J. Fluid Mech. 559 (2006) 57–80.
[43] P. Bonneton, N. Bruneau, F. Marche, B. Castelle, Large-scale vorticity generation due to dissipating waves in the surf zone, DCDS-B 13 (4) (2010) 729–738. doi:10.3934/dcdsb.2010.13.729.
[44] Lord Rayleigh, On waves, Philos. Mag. 1 (1876) 257–279.
[45] K. Guizien, E. Barthlemy, Accuracy of solitary wave generation by a piston wave maker, J. Hydraul. Res. 40 (3) (2002) 321–331.
[46] Y.A. Li, J.M. Hyman, W. Choi, A numerical study of the exact evolution equations for surface waves in water of finite depth, Stud. Appl. Math. 113 (3) (2004) 303–324.
[47] F. Serre, Contribution à l'étude des écoulements permanents et variables dans les canaux, Houille Blanche 6 (1953) 830–872.
[48] G.A. El, R.H.J. Grimshaw, N.F. Smyth, Unsteady undular bores in fully nonlinear shallow-water theory, Phys. Fluids 18 (2006) 027104.
[49] J.D. Carter, R. Cienfuegos, The kinematics and stability of solitary and cnoidal wave solutions of the Serre equations, Eur. J. Mech. B, in press (doi:10.1016/j.euromechflu.2010.12.002).
[50] R. Cienfuegos, E. Barthélemy, P. Bonneton, A wave-breaking model for Boussinesq-type equations including mass-induced effects, J. Waterway Port Coast Ocean Eng. 136 (2010) 10–26.
[51] F.C.K. Ting, J.T. Kirby, Observation of undertow and turbulence in a laboratory surf zone, Coast. Eng. 24 (1994) 51–80.
[52] M.H. Kobayashi, On a class of Padé finite volume methods, J. Comput. Phys. 156 (1999) 137–180.
[53] C. Lacor, S. Smirnov, M. Baelmans, A finite volume formulation of compact central schemes on arbitrary structured grids, J. Comput. Phys. 198 (2004) 535–566.
[54] E. Mignot, R. Cienfuegos, On the application of a Boussinesq model to river flows including shocks, Coast. Eng. 56 (2009) 23–31.
[55] P.J. Lynett, T.R. Wu, P.L.F. Liu, Modeling wave runup with depth-integrated equations, Coast. Eng. 46 (2002) 89–107.
[56] R. Cienfuegos, E. Barthelemy, P. Bonneton, X. Gondran, Analysis of nonlinear surf zone wave properties as estimated from Boussinesq modelling: random waves and complex bathymetries, Proc. 30th Int. Conf. on Coast. Eng. 1 (2006) 360–371.
[57] L. Duarte, R. Cienfuegos, E. Hernandez, Estudio experimental del mecanismo de generacion de ondas largas en una playa de pendiente suave, in: XXIII Congreso Latinoamericano de Hidraulica, Cartagena de Indias, Colombia, 2008.
[58] R. Cienfuegos, L. Duarte, L. Suarez, P. Catalán, Numerical computation of infragravity wave dynamics and velocity profiles using a fully non-linear Boussinesq model, in: Proceedings of the International Conference on Coastal Engineering, North America, 1, Jan. 2011. Available at: http://journals.tdl.org/ICCE/article/view/1885 (accessed 21.03.11).
[59] E. Godlewski, P.-A. Raviart, Numerical approximation of hyperbolic systems of conservation laws, in: Applied Mathematical Sciences, vol. 118, Springer, 1996.
[60] C. Berthon, F. Marche, A positive preserving high order VFRoe scheme for shallow water equations: a class of relaxation schemes, SIAM J. Sci. Comput. 30 (5) (2008) 2587–2612.
[61] E. Audusse, F. Bouchut, M.-O. Bristeau, R. Klein, B. Perthame, A fast and stable well-balanced scheme with hydrostatic reconstruction for shallow water flows, J. Comput. Phys. 25 (6) (2004) 2050–2065.
[62] F. Marche, P. Bonneton, A simple and efficient well-balanced scheme for 2D bore propagation and run-up over a sloping beach, Proc. 30th Int. Conf. on Coast. Eng. 1 (2006) 998–1010.
[63] J.J. Sampson, A. Easton, M. Singh, Moving boundary shallow water flow in a region with quadratic bathymetry, ANZIAM J. 49 (2007) 666–680.
[64] M. Tissier, P. Bonneton, F. Marche, F. Chazel, D. Lannes, Serre Green–Naghdi modelling of wave transformation breaking and run-up using a high-order finite-volume finite-difference scheme, in: Proc. 32nd Int. Conf. on Coast. Eng., Shanghai, China, 2010.
[65] C.E. Synolakis, The runup of solitary waves, J. Fluid Mech. 185 (1987) 523–545.